Journal of Science and Technology – Engineering and Technology for Sustainable Development
Volume 36, Issue 1, March 2026, 087-096

Dynamical Analysis of a Predator-Prey Model with Predator Intraspecific Competition, Prey Group Defense, Wind Flow, and Harvesting Effort

Nguyen Phuong Thuy*, Van Duc An, Trieu Thi Thoa
Hanoi University of Science and Technology, Ha Noi, Vietnam
**Corresponding author email: thuy.nguyenphuong@hust.edu.vn*

Abstract

This study introduces a novel predator-prey model that integrates the effects of predator intraspecific competition, prey group defense mechanisms, wind flow, and harvesting effort. The model employs a modified Holling type II functional response to capture the complexity of prey-predator interactions under environmental and anthropogenic influences. We establish the model's positivity and boundedness and derive conditions for the local and global stability of equilibrium points. Hopf bifurcation analysis reveals that both wind intensity and harvesting effort significantly affect system stability. Numerical simulations demonstrate that while mild wind flow can stabilize the system with minimal group defense, increased wind intensity enhances overall system stability. Furthermore, harvesting pressure and intraspecific competition contribute to stability regardless of wind strength. The analysis also shows that intraspecific competition and harvesting effort are positively correlated with prey density and negatively correlated with predator density at equilibrium.

Keywords: Group defense, harvesting effort, hopf bifurcation, intraspecific competition, stability analysis, prey-predator model, wind flow.

1. Introduction

In recent decades, the study of predator-prey dynamics has advanced considerably, with a growing emphasis on both biotic and abiotic factors that influence ecological interactions. Traditional models have primarily focused on biological mechanisms such as foraging behavior, group defense, and interspecific and intraspecific competition. However, there is increasing recognition of the significant role played by abiotic elements and anthropogenic activities in shaping ecosystem behavior.

Abiotic factors–including temperature, precipitation, light availability, and wind flow–exert profound effects on species distribution, movement, and interaction patterns [1–3]. Wind flow has emerged as a particularly influential variable due to its capacity to alter dispersal routes, migration behavior, and foraging efficiency. Despite its ecological relevance, the integration of wind dynamics into predator-prey models remains limited. Notable contributions by Barman *et al.* and Takyi *et al.* have begun to address this gap by incorporating wind effects and prey refuge into dynamical systems [4–6].

In parallel, human activities such as harvesting have become dominant forces in ecological systems, often surpassing natural biotic and abiotic influences. Incorporating harvesting effort into population models is essential for understanding the broader implications of human intervention on species persistence and ecosystem stability [7–9].

Wind flow dynamics can influence resource availability and accessibility, affecting human harvesting practices. Conversely, human harvesting activities may cause population declines, leading to changes in ecological dynamics and ultimately impacting resource distribution and ecosystem structure.

This study extends previous work by developing a comprehensive predator-prey model that incorporates wind flow as an abiotic factor and harvesting effort as a human influence. The model also accounts for prey group defense and predator intraspecific competition, offering a more holistic view of ecological dynamics. Through mathematical analysis and numerical simulations, we aim to elucidate the complex interplay between environmental forces, biological traits, and anthropogenic pressures.

The remainder of this paper is organized as follows: Section 2 introduces the mathematical model and underlying ecological assumptions. Section 3 presents the analytical results, including positivity, boundedness, and stability analyses, as well as Hopf bifurcation conditions. Section 4 provides numerical simulations to support the theoretical findings and discusses their ecological implications. Finally, Section 5 concludes the study with key insights and potential directions for future research.

2. The Mathematical Model

To investigate the combined effects of wind flow, intraspecific competition among predators, prey group

p-ISSN 3093-3242
e-ISSN 3093-3579
https://doi.org/10.51316/jst.188.etsd.2026.36.1.11
Received: Mar 22, 2025; Revised: May 29, 2025;
Accepted: Jun 16, 2025; Online: Feb 6, 2026.

defense, and harvesting effort, we propose a system of nonlinear ordinary differential equations. The model captures the dynamics of prey and predator populations over time and is formulated as follows:

$$\begin{cases} \dfrac{\mathrm{d}u}{\mathrm{d}t} = ru\left(1-\dfrac{u}{k}\right) - \dfrac{\alpha_1 uv}{1+w+bu+\dfrac{bwu}{1+w}} \\ \dfrac{\mathrm{d}v}{\mathrm{d}t} = \dfrac{\alpha_2 uv}{1+w+bx+\dfrac{bwu}{1+w}} - dv - hv - \gamma v^2 \end{cases} \quad (1)$$

with initial conditions:

$$u(0) > 0, v(0) > 0 \quad (2)$$

Here, all parameters are assumed to be non-negative. The variables and parameters are defined in Table 1. This model incorporates a modified Holling type II functional response, adjusted to reflect the influence of wind flow and group defense on predation efficiency. The prey population grows logistically, while the predator population is subject to natural mortality, harvesting, and density-dependent competition. The interaction terms are modulated by environmental and behavioral factors, making the model suitable for analyzing complex ecological dynamics under both natural and anthropogenic influences.

Table 1. Model parameters with ecological descriptions

Parameters /Variables	Description
$u(t)$	Prey population density at time *t*
$v(t)$	Predator population density at time *t*
r	Intrinsic growth rate of the prey
k	Carrying capacity of the prey
w	Intensity of wind flow
α_1	Predation rate coefficient
α_2	Conversion efficiency of prey into predator biomass
b	Group defense coefficient of the prey
d	Natural mortality rate of the predator
h	Harvesting effort on the predator population
γ	Intraspecific competition coefficient among predators

3. Model Analysis

This section presents a comprehensive analysis of the proposed predator-prey model, focusing on the positivity and boundedness of solutions, the existence and stability of equilibrium points, and the conditions under which Hopf bifurcation may occur.

3.1. Positivity and Boundedness of Solutions

To ensure biological feasibility, it is essential to demonstrate that the solutions of the system remain non-negative and bounded for all time $t > 0$.

Theorem 3.1: *All solutions of the system with initial conditions* $u(0) > 0$, $v(0) > 0$ *remain non-negative for all* $t > 0$.

Proof:

The right-hand side of the system is continuous and locally Lipschitz in the first quadrant $P = \{(u, v): u, v \geq 0\}$, ensuring the existence and uniqueness of solutions. By integrating the system, it can be shown that both $u(t)$ and $v(t)$ remain non-negative for all $t > 0$.

$$\begin{aligned} &u(t) \\ &= u(0)exp\left\{\int_0^t \left[r\left(1-\frac{u(s)}{k}\right)\right.\right. \\ &\left.\left. - \frac{\alpha_1 v(s)}{1+w+bu(s)+\dfrac{bwu(s)}{1+w}}\right] ds\right\} \\ &\geq 0 \end{aligned} \quad (3)$$

$$v(t) = v(0)exp\left\{\int_0^t \left[\frac{\alpha_2 u(s)}{1+bu(s)+w+\frac{bwu(s)}{1+w}} - d - h - \gamma v(s)\right] ds\right\} \geq 0 \quad (4)$$

Theorem 3.2: *All solutions of the system are bounded for all* $t > 0$.

Proof:

$$\text{Let } Q(t) = u(t) + \frac{\alpha_1}{\alpha_2} v(t),\ t \geq 0 \quad (5)$$

By differentiating Q along the trajectories of the system, we obtain:

$$\begin{aligned} \frac{dQ}{dt} &= \frac{du(t)}{dt} + \frac{\alpha_1}{\alpha_2}\frac{dv(t)}{dt} \\ &= ru\left(1-\frac{u}{k}\right) \\ &\quad - \frac{(d+h)\alpha_1}{\alpha_2} v \end{aligned} \quad (6)$$

Choosing $\delta \in \mathbb{R}^+$, such that $\delta \leq d + h$, we get,

$$\begin{aligned} \frac{\mathrm{d}Q}{\mathrm{d}t} + \delta Q &= (r+\delta)u - \frac{\mathrm{r}u^2}{k} \\ &\quad - \frac{\alpha_1 v}{\alpha_2}(d+h+\delta) \\ &\leq (r+\delta)u - \frac{\mathrm{r}u^2}{k} \leq \frac{k(r+\delta)^2}{4r} = M \end{aligned} \quad (7)$$

Therefore,

$$\frac{\mathrm{d}Q}{\mathrm{d}t} + \delta Q \le M \Leftrightarrow Q(t) \le \frac{M}{\delta} + Q(u_0, v_0)e^{-\delta t} \quad (8)$$

$$\Leftrightarrow 0 \le Q \le \frac{M}{\delta} + Q(u_0, v_0)e^{-\delta t}$$

$Q(t)$ is bounded above by $\frac{M}{\delta}$ when $t \to \infty$, therefore, both $u(t)$and $v(t)$ are bounded.

3.2. Equilibrium Points and Stability Analysis

The equilibrium points of the system are obtained by setting the right-hand sides of the differential equations to zero:

$$\begin{cases} ru\left(1 - \frac{u}{k}\right) - \frac{\alpha_1 uv}{1 + w + bu + \frac{bwu}{1+w}} = 0 \\ \frac{\alpha_2 uv}{1 + w + bx + \frac{bwu}{1+w}} - dv - hv - \gamma v^2 = 0 \end{cases} \quad (9)$$

Solving the system of equations (9) yields three potential equilibrium points:

1. The trivial equilibrium point $E_0 = (0,0)$ which always exists, represents the situation where both species will go extinct.

2. The axial equilibrium point $E_1 = (k, 0)$ always exists. This equilibrium represents the situation in which the prey grows to the environment's carrying capacity, and the predator goes extinct.

3. Coexistence equilibrium point $E^* = (u^*, v^*)$, where

$v^* = \frac{r}{\alpha_1}\left(1 + bu^* + w + \frac{bwu^*}{1+w}\right)$ and u^* is the solution of the following equation:

$$A_1 u^3 + A_2 u^2 + A_3 u + A_4 = 0 \quad (10)$$

where

$$A_1 = \frac{\gamma r}{k}\frac{b^2(1+2w)^2}{(1+w)^2},$$

$$A_2 = \gamma r\left[\frac{2b(1+2w)}{k} - \frac{b^2(1+2w)^2}{(1+w)^2}\right],$$

$$A_3 = \gamma r\left[\frac{(1+w)^2}{k} - 2b(1+2w)\right] + \alpha_1\alpha_2 - \alpha_1 b(d + h)\frac{(1+2w)}{1+w},$$

$$A_4 = -[\gamma r(1+w)^2 + \alpha_1(d+h)(1+w)].$$

E^* exists if u^* is positive. This equilibrium represents the situation where both species exist.

3.2.1. Local stability analysis

We begin by examining the local stability of the equilibrium points through the system's Jacobian matrix. The right-hand side expression of system (1) is expressed separately as the following function:

$$F(u,v) = ru\left(1 - \frac{u}{k}\right) - \frac{\alpha_1 uv}{1 + w + bu + \frac{bwu}{1+w}},$$

$$G(u,v) = \frac{\alpha_2 uv}{1 + w + bu + \frac{bwu}{1+w}} - dv - hv - \gamma v^2.$$

The Jacobian matrix of the system (1) is as follows

$$B(u,v) = \begin{pmatrix} B_{11} & B_{12} \\ B_{21} & B_{22} \end{pmatrix},$$

where

$$B_{11} = \frac{\partial F}{\partial u} = r\left(1 - \frac{2u}{k}\right) - \frac{\alpha_1(1+w)v}{\left(1 + bu + w + \frac{bwu}{1+w}\right)^2},$$

$$B_{12} = \frac{\partial F}{\partial v} = -\frac{\alpha_1 u}{1 + w + bu + \frac{bwu}{1+w}},$$

$$B_{21} = \frac{\partial G}{\partial u} = \frac{\alpha_2(1+w)v}{\left(1 + w + bu + \frac{bwu}{1+w}\right)^2},$$

$$B_{22} = \frac{\partial G}{\partial v} = \frac{\alpha_2 u}{1 + w + bu + \frac{bwu}{1+w}} - d - h - 2\gamma v.$$

Theorem 3.3 *The trivial equilibrium points $E_0 = (0,0)$ is always unstable.*

Proof:

The Jacobian matrix corresponding to the equilibrium point E_0:

$$B(0,0) = \begin{pmatrix} r & 0 \\ 0 & -d - h \end{pmatrix} \quad (11)$$

The Jacobian matrix $B(0,0)$ have 2 eigenvalues:

$\lambda_1 = r > 0;$

$\lambda_2 = -d - h < 0.$

Thus, using the first Lyapunov method, E_0 is always unstable; therefore, system (1) exhibits unstable behavior around the trivial equilibrium point E_0.

Theorem 3.4 *The axial equilibrium point $E_1 = (k, 0)$ is locally asymptotically stable if the following condition holds:*

$$\alpha_2 k < (d+h)(1+w) + bk(d+h)\left(1 + \frac{w}{1+w}\right) \quad (12)$$

Proof:

At $E_1 = (k, 0)$, the associated Jacobian matrix is: $B(k,0) = \begin{pmatrix} -\mathrm{r} & 0 - \frac{\alpha_1 k}{1+w+bk+\frac{bwk}{1+w}} \\ 0 & \frac{\alpha_2 k}{1+w+bk+\frac{bwk}{1+w}} - d - h \end{pmatrix}$ (13)

The Jacobian matrix has 2 eigenvalues:

$$\lambda_1 = -r < 0,$$

$$\lambda_2 = \frac{\alpha_2 k}{1+w+bk+\frac{bwk}{1+w}} - d - h.$$

Using the first Lyapunov method, the condition for E_1 to be locally asymptotically stable is $\lambda_2 < 0$ then we have the condition (12).

Theorem 3.5. *The coexistence equilibrium point $E^* = (u^*, v^*)$ is locally asymptotically stable if*

$$\left(1 - \frac{2u^*}{k}\right) r - \frac{\alpha_1 (1+w) v^*}{\left(1+w+bu^* + \frac{bwu^*}{1+w}\right)^2} < 0 \qquad (14)$$

Proof:

At equilibrium point E^*, the associated Jacobian matrix is:

$$B(u^*, v^*) = \begin{pmatrix} B_{11}^* & B_{12}^* \\ B_{21}^* & B_{22}^* \end{pmatrix} \qquad (15)$$

where $B_{11}^*, B_{12}^*, B_{21}^*, B_{22}^*$ are the corresponding expression of $B_{11}, B_{12}, B_{21}, B_{22}$ at coexistence equilibrium point E^*. The characteristic equation of this Jacobian matrix is:

$$\lambda^2 - (B_{11}^* + B_{22}^*)\lambda + B_{11}^* B_{22}^* - B_{12}^* B_{21}^* = 0 \qquad (16)$$

where

$$B_{11}^* = r\left(1 - \frac{2u^*}{k}\right) - \frac{\alpha_1 (1+w) v^*}{\left(1+w+bu^* + \frac{bwu^*}{1+w}\right)^2},$$

$$B_{12}^* = -\frac{\alpha_1 u^*}{1+w+bu^* + \frac{bwu^*}{1+w}},$$

$$B_{21}^* = \frac{\alpha_2 (1+w) v^*}{\left(1+w+bu^* + \frac{bwu^*}{1+w}\right)^2},$$

$$B_{22}^* = \frac{\alpha_2 u^*}{1+w+bu^* + \frac{bwu^*}{1+w}} - d - h - 2\gamma v^* = -\gamma v^*.$$

Equation (4) has two roots with negative real parts if

$$\begin{cases} B_{11}^* + B_{22}^* < 0 \\ B_{11}^* B_{22}^* - B_{12}^* B_{21}^* > 0. \end{cases}$$

It is obvious that $B_{12}^* < 0, B_{22}^* < 0$ and $B_{21}^* > 0$.

Hence, if $B_{11}^* < 0$ or we have the condition (14), then the following inequalities will be satisfied:

$B_{11}^* + B_{22}^* < 0$, $B_{11}^* B_{22}^* - B_{12}^* B_{21}^* > 0$. Using the first Lyapunov method, we obtain conditions under which E^* is locally asymptotically stable.

3.2.2. Global stability of the coexistence equilibrium

Theorem 3.6 *Coexistence equilibrium point $E^* = (u^*, v^*)$ is globally asymptotically stable if*

$$u > u^*, v > v^* \qquad (17)$$

and the following condition is satisfied:

$$\frac{r}{k} > \frac{b\alpha_1 \left(1 + \frac{w}{1+w}\right) v^*}{(1+w)\left[1+w+b\left(1+\frac{w}{1+w}\right)u^*\right]} \qquad (18)$$

Proof:

Firstly, a Lyapunov function is constructed as follows:

$$L(u,v) = \alpha_1 \int_{u^*}^{u} \left(\frac{u-u^*}{u}\right) du + \alpha_2 \int_{v^*}^{v} \left(\frac{v-v^*}{v}\right) dv \qquad (19)$$

where α_1 and α_2 are properly chosen positive constants.

By differentiating $C(u,v)$ with respect to t, we obtain:

$$\frac{dL}{dt} = \alpha_1 \left(\frac{u-u^*}{u}\right)\frac{du}{dt} + \alpha_2 \left(\frac{v-v^*}{v}\right)\frac{dv}{dt}$$

$$= \alpha_1 (u-u^*)\left[\frac{1}{u}\frac{du}{dt} - \frac{1}{u^*}\left(\frac{du}{dt}|_{u=u^*}\right)\right] +$$

$$+\alpha_2 (v-v^*)\left[\frac{1}{v}\frac{dv}{dt} - \frac{1}{v^*}\left(\frac{dv}{dt}|_{v=v^*}\right)\right]$$

$$= \alpha_1 (u-u^*)\left[\left(-\frac{r}{k}\right)(u-u^*) - \frac{\alpha_1 v}{1+bu+w+\frac{bwu}{1+w}} + \right.$$

$$\left. + \frac{\alpha_1 v^*}{1+w+bu^*+\frac{bwu^*}{1+w}}\right] + \alpha_2 (v-v^*)\left[-\frac{\alpha_2 u}{1+bu+w+\frac{bwu}{1+w}} - \right.$$

$$\left. - \frac{\alpha_2 u^*}{1+w+bu^*+\frac{bwu^*}{1+w}} - \gamma(v-v^*)\right] \qquad (20)$$

Let

$$g(u) = 1 + w + bu + \frac{bwu}{1+w} \qquad (21)$$

from which we derive:

$$\frac{dL}{dt} = \alpha_1 (u-u^*)\left(-\frac{r}{k}(u-u^*) - \frac{\alpha_1 v}{g(u)} + \frac{\alpha_1 v^*}{g(u^*)}\right)$$

$$+ \alpha_2 (v-v^*)\left(\frac{\alpha_2 u}{g(u)} + \frac{\alpha_2 u^*}{g(u^*)}\right).$$

$$= \alpha_1 (u-u^*)\left(-\frac{r}{k}(u-u^*) - \frac{\alpha_1 v}{g(u)} + \frac{\alpha_1 v^*}{g(u)}\right.$$

$$\left. - \frac{\alpha_1 v^*}{g(u)} + \frac{\alpha_1 v^*}{g(u^*)}\right)$$

$$+\alpha_2(v-v^*)\left(\frac{\alpha_2 u}{g(u)}-\frac{\alpha_2 u^*}{g(u)}+\frac{\alpha_2 u^*}{g(u)}-\frac{\alpha_2 u^*}{g(u^*)}-\gamma(v-v^*)\right)$$

$$=\alpha_1(u-u^*)\left[\left(-\frac{r}{k}\right)(u-u^*)-\alpha_1\frac{v-v^*}{g(u)}+\right.$$
$$\left.+\frac{b\alpha_1\left(1+\frac{w}{1+w}\right)v^*(u-u^*)}{g(u)g(u^*)}\right]+\frac{\alpha_2\alpha_2(1+w)(u-u^*)(v-v^*)}{g(u)g(u^*)}-$$
$$-\alpha_2\gamma(v-v^*)^2$$

$$=-\alpha_1(u-u^*)^2\left[\frac{r}{k}-\frac{b\alpha_1\left(1+\frac{w}{1+w}\right)v^*}{g(u)g(u^*)}\right]+$$
$$+\frac{(u-u^*)(v-v^*)}{g(u)g(u^*)}[\alpha_2\alpha_2(1+w)-\alpha_1\alpha_1 g(u^*)]-$$
$$-\alpha_2\gamma(v-v^*)^2 \quad (22)$$

Choosing

$$\alpha_1=\frac{\alpha_2\alpha_2(1+w)}{\alpha_1 g(u^*)} \quad (23)$$

we get:

$$\frac{dL}{dt}=-\alpha_1(u-u^*)^2\left[\frac{r}{k}-\frac{b\alpha_1\left(1+\frac{w}{1+w}\right)v^*}{g(u)g(u^*)}\right] \quad (24)$$

Imposing the condition

$$\frac{r}{k}>\frac{b\alpha_1\left(1+\frac{w}{1+w}\right)v^*}{(1+w)\left[1+w+b\left(1+\frac{w}{1+w}\right)u^*\right]}, \text{ t} \quad (25)$$

we have $\frac{dC}{dt}<0$. Using Lyapunov's second method along with LaSalle's invariance principle, the equilibrium point E^* is globally asymptotically stable. The proof is complete.

3.3. Hopf Bifurcation

To explore the emergence of periodic solutions in the system, we analyze the conditions under which a Hopf bifurcation occurs at the coexistence equilibrium point E^*.

Theorem 3.7: *A Hopf bifurcation occurs at* $w=w^*$ *if the following conditions are satisfied:*

$$i.\ B_{11}^*+B_{22}^*=0; \quad (26)$$

$$ii.\ B_{11}^*B_{22}^*-B_{12}^*B_{21}^*>0; \quad (27)$$

$$iii.\ \frac{\partial(B_{11}^*+B_{22}^*)}{\partial t}\neq 0. \quad (28)$$

Proof: By substituting a complex eigenvalue $\lambda=x+iy$ into the characteristic equation and separating real and imaginary parts, we derive the conditions under which a pair of purely imaginary eigenvalues emerges, indicating the onset of a Hopf bifurcation.

$$x=-\frac{a_1}{2},$$

$$x|_{w=w^*}=0 \text{ or } a_1|_{w=w^*}=0, \quad (29)$$

and

$$\frac{dx}{dw}|_{w=w^*}\neq 0 \text{ or } \frac{da_1}{dw}|_{w=w^*}\neq 0. \quad (30)$$

3.4. Optimal Harvesting Effort

To determine the optimal level of harvesting that maximizes yield without destabilizing the system, we analyze the Maximum Sustainable Yield (MSY) under the assumption that intraspecific competition among predators is negligible.

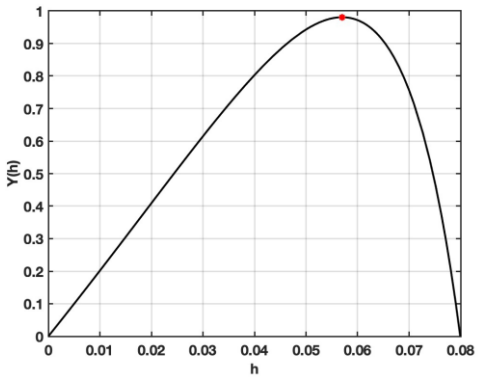

Fig. 1. Graph of $Y(h)$ with the parameters provided in Table 2

Table 2. Parameter sets for the stable of each equilibrium point

Parameter	E_1	E^*
r	0.8	0.8
k	10	10
w	20	20
b	6	2
α_1	0.9	0.9
α_2	0.6	0.6
d	0.02	0.02
h	0.03	0.03
γ	0.002	0.002

Theorem 3.8: *The MSY is achieved when the harvesting effort h reaches the value:*

$$h=\frac{h_1}{h_2} \quad (31)$$

where:

$$h_1=k[\alpha_2(1+w)-bd(1+2w)]^2$$
$$-d(1+w)^2[\alpha_2(1+w)-bd(1+2w)], \quad (32)$$

$$h_2=[kb(1+2w)+2(1+w)^2][\alpha_2(1+w)-$$
$$bd(1+2w)]+bd(1+2w)(1+w)^2. \quad (33)$$

Proof:

By expressing the equilibrium predator density $E^* = (u^*, v^*)$, as a function of h, the yield function $Y(h) = hv^*$ is derived.

$$u^* = \frac{(d+h)(1+w)^2}{\alpha_2(1+w) - bd(1+2w)},$$

$$v^* = \frac{r\alpha_2(1+w)^2 k[\alpha_2(1+w) - b(d+h)(1+2w)]}{\alpha_1 k[\alpha_2(1+w) - b(d+h)(1+2w)]^2} - \frac{r\alpha_2(1+w)^4(d+h)}{\alpha_1 k[\alpha_2(1+w) - b(d+h)(1+2w)]^2}.$$

$$Y(h) = hv^*$$

$$= h\frac{r\alpha_2(1+w)^2 k[\alpha_2(1+w) - b(d+h)(1+2w)]}{\alpha_1 k[\alpha_2(1+w) - b(d+h)(1+2w)]^2} - h\frac{r\alpha_2(1+w)^4(d+h)}{\alpha_1 k[\alpha_2(1+w) - b(d+h)(1+2w)]^2}.$$

Differentiating $Y(h)$ with respect to h and solving $Y'(h) = 0$, yields the optimal harvesting effort.

$$\frac{\mathrm{d}Y}{\mathrm{d}h} = \frac{r\alpha_2(1+w)^2}{k\alpha_1}\left[\frac{k}{N} + \frac{kbh(1+2w) - (1+w)^2(2d+h)}{N^2} - \frac{2b(1+2w)(1+w)^2(d+h)h}{N^3}\right],$$

where $N = \alpha_2(1+w) - b(d+h)(1+2w)$. The behavior of the function $Y(h)$ is illustrated in Fig. 1.

$$Y'(h) = \frac{r\alpha_2(1+w)^2}{k\alpha_1}\frac{k}{N} + \frac{kbh(1+2w)}{N^2} - \frac{(1+w)^2(2d+h)}{N^2} - \frac{2b(1+2w)(1+w)^2(d+h)h}{N^3} = 0.$$

$$\Leftrightarrow kN^2 + [kbh(1+2w) - (1+w)^2(2h+d)]N - 2bh(d+h)(1+2w)(1+w)^2 = 0.$$

Replacing $N = \alpha_2(1+w) - b(d+h)(1+2w)$, we obtain:

$$h = \frac{h_1}{h_2} \quad (34)$$

where:

$$h_1 = k[\alpha_2(1+w) - bd(1+2w)]^2 - d(1+w)^2[\alpha_2(1+w) - bd(1+2w)], \quad (35)$$

$$h_2 = [kb(1+2w) + 2(1+w)^2][\alpha_2(1+w) - bd(1+2w)] + bd(1+2w)(1+w)^2 \quad (36)$$

From the equations (34), (35), (36), we obtain the equation (31).

4. Numerical Simulations and Discussion

To validate the theoretical results and explore the dynamic behavior of the system under various parameter settings, we conducted numerical simulations using the parameter values listed in Table 2. These simulations illustrate the stability of the axial equilibrium E_1 and the coexistence equilibrium E^*, as well as the effects of key ecological and environmental factors. Although the conditions of Theorem (3.4, 3.5, and 3.6) are complex, it is still possible to select a set of parameters that satisfy these conditions, as presented in Table 2. This demonstrates that the parameter set is non-empty. The chosen parameter sets satisfy the local stability conditions of the equilibrium points E_1 and E^*, and are used to conduct simulations with varying population sizes for each species (see Fig. 2 and Fig. 3).

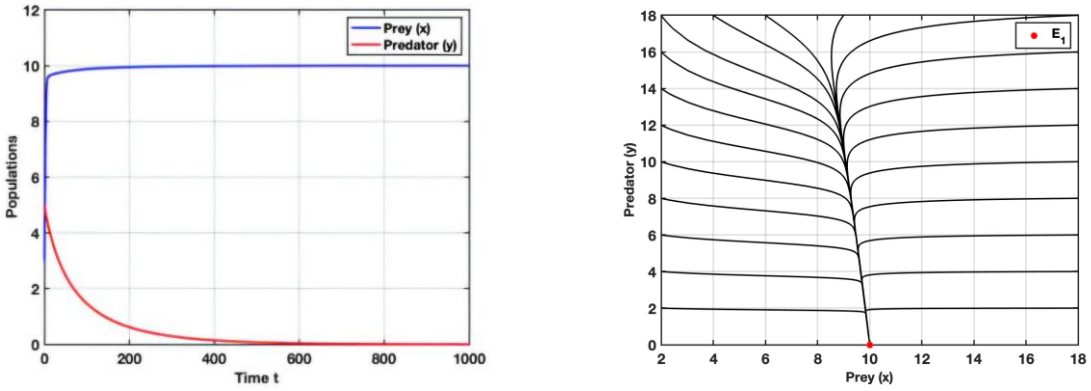

a) Time evolution of population densities b) Phase portrait of the dynamical system

Fig. 2. The behavior of the system (1) in case of stable equilibrium point E_1

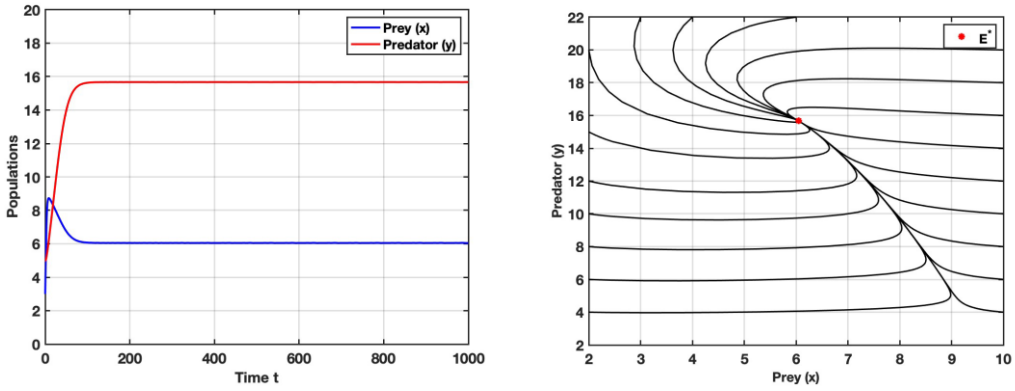

a) Time evolution of population densities b) Phase portrait of the dynamical system

Fig. 3. The behavior of the system (1) in case of stable equilibrium point E^*

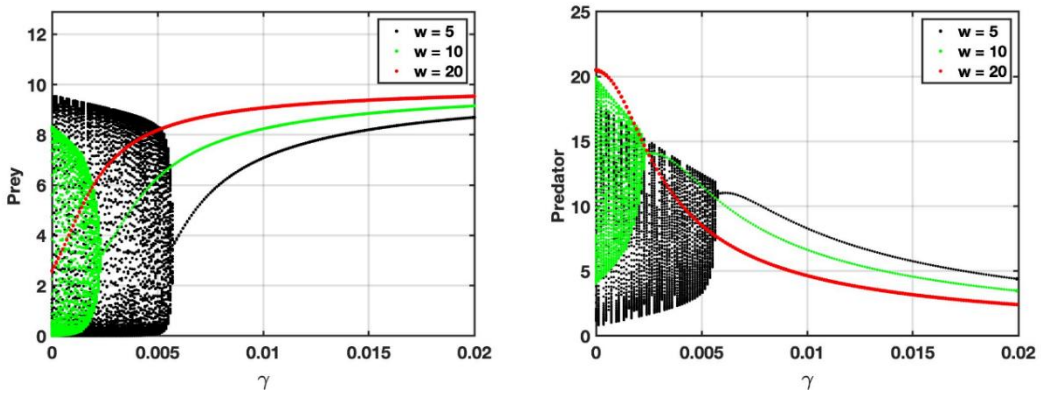

a) Prey population density b) Predator population density

Fig. 4. Hopf bifurcation diagram with changing intensity of intraspecific competition γ at different intensity of wind flow w

4.1. Effect of Intraspecific Competition

Fig. 4 illustrates the dynamical system's behavior as the predator's intraspecific competition rate varies under different wind flow intensities. When the wind flow intensity is set to w be equal to5 and the value of predator intraspecific competitive γ is less than 0.0065, the dynamical system exhibits a limit cycle around coexistence equilibrium point E^*. When γ is greater than 0.0065, the system transitions from stability at the coexistence equilibrium point to stability at the boundary equilibrium point. When the value of w is increased, the instability of the dynamical system is reduced, and the population density of prey increases while the population density of predator decreases. When w is equal to 20, we can see that the system transitions from stability at the coexistence equilibrium point to stability at the boundary equilibrium point without Hopf bifurcation.

4.2. Effect of Harvesting Effort

Fig. 5 shows the dynamical system's behavior when the harvesting effort value changes at different intensities of wind flow. When the wind flow intensity w is set to value 5, the dynamical system exhibits population instability when the harvesting effort satisfies h is less than0.075 and stability when h is greater than 0.075. When h is greater than 0.12, the system transitions from stability around the equilibrium point to stability around the boundary equilibrium point. It can be observed that humans' excessive hunting of animal species can drive the species to extinction. The dynamical system exhibits analogous behavior when the value of w is increased to 10. However, the range of values for h that cause instability is reduced, and the amplitude of population oscillations for both species decreases accordingly. When the wind flow strength w takes the value of 20, the system becomes stable and no longer affected by h.

4.3. Effect of Wind Flow

In Fig. 6, simulations show the critical role of the wind factor in the dynamical system. Unstable behavior of the model system is observed as w increases from 0

to 10.9, and the oscillations in prey and predator populations become progressively damped. When the strength of wind flow w is low, predators exhibit typical predator patterns, occasionally consuming a large amount of prey. Over time, this leads to a reduction in prey offspring, causing food shortages for predators and resulting in oscillatory dynamics in both populations. However, as w increases, predators find it increasingly difficult to detect prey, leading to smaller oscillations in the population dynamics. When w surpasses the critical point 10.9, the model system exhibits stable behavior around the coexistence equilibrium point. However, if the wind flow strength becomes excessively high, the system's stability shifts from the coexistence equilibrium to the axial equilibrium point. This occurs because, under high wind flow conditions, predators cannot detect prey, leading to the eventual extinction of the predator population. Consequently, the prey population grows unchecked, reaching the environmental carrying capacity.

4.4. Effect of Prey Group Defense

Fig. 7 shows the dynamical systems behavior when the value of prey group defense changes at different intensities of wind flow. When the strength of wind flow is fixed at w be equal to 5, the dynamical system exhibits stability around the equilibrium point while the value of the parameter b varies in the range from 0 to 0.45. However, once the value of b surpasses the threshold of 0.45, the dynamical system becomes unstable, leading to the emergence of limit cycles with large amplitude oscillations for each species. If the value of b continues to increase beyond 3.2, the dynamical system regains stability. The system remains stable as the value of b increases; however, when b is greater than 6.3, instead of being stable around the equilibrium point, the dynamical system stabilizes around the axial equilibrium point. This means that the predator species becomes extinct, while the prey population grows to reach the environment's maximum carrying capacity. This scenario aligns with natural dynamics, as excessive defensive capabilities in prey can hinder successful predation, ultimately leading to the predator's extinction. When we fix w be equal to 10, the dynamical system exhibits similar behavior as when w is equal to5. However, the range of values for b that causes instability is reduced, and the amplitude of oscillations for both species during instability decreases significantly. When w is equal to 20, the dynamical system remains stable, and its behavior becomes independent of the parameter b.

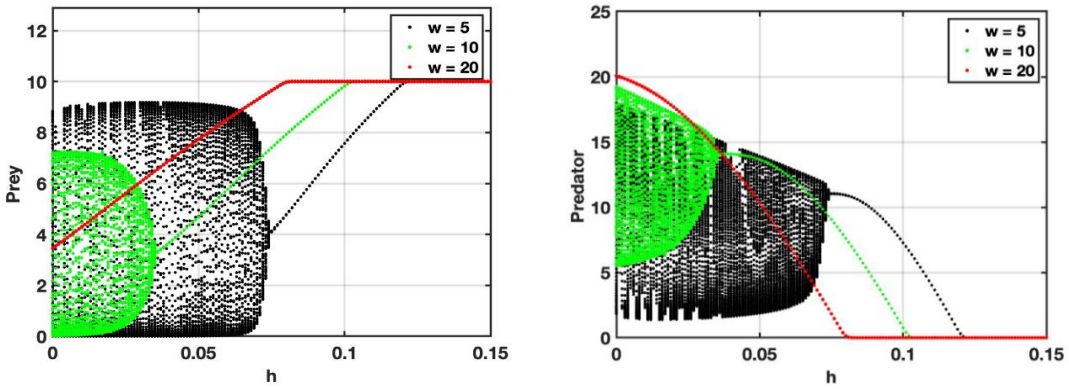

a) Prey population density b) Predator population density

Fig. 5. Hopf bifurcation diagram with changing harvesting effort h at different intensity of wind flow w

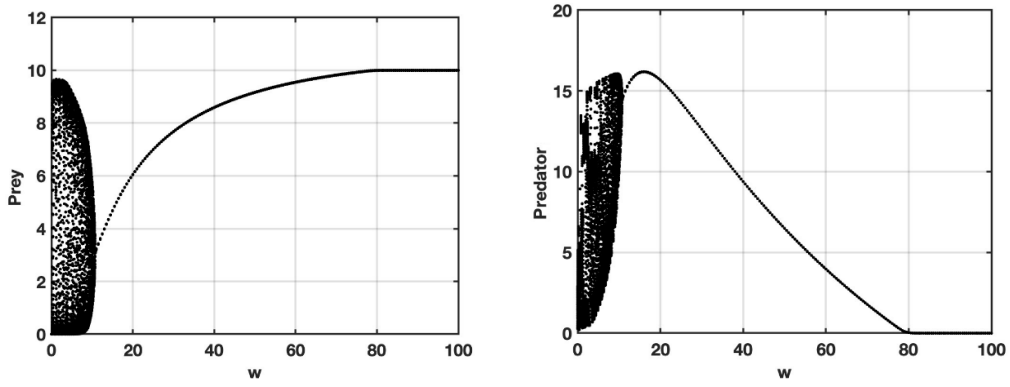

a) Prey population density b) Predator population density

Fig. 6. Hopf bifurcation diagram with changing the intensity of wind flow w

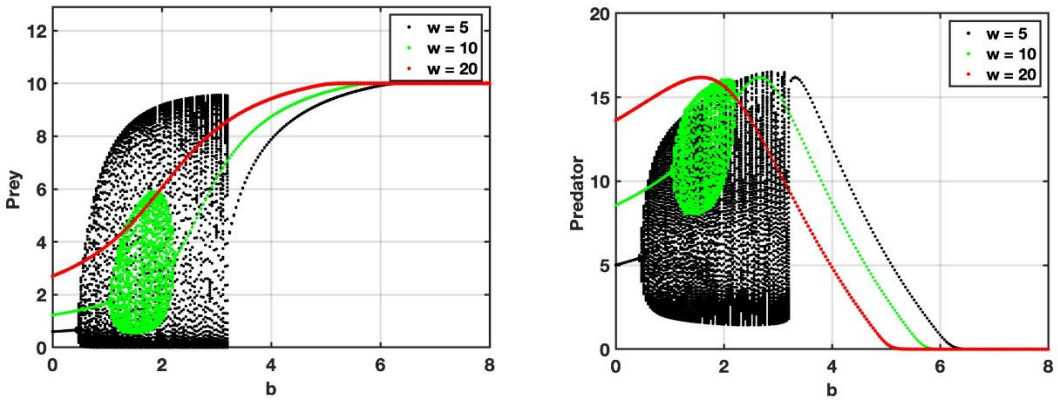

a) Prey population density b) Predator population density

Fig. 7: Hopf bifurcation diagram with changing prey group defense b at different intensity of wind flow w

5. Conclusion

In this study, we developed and analyzed a nonlinear predator-prey model that incorporates the effects of wind flow, prey group defense, predator intraspecific competition, and harvesting effort. The model extends classical predator-prey dynamics by integrating both environmental and anthropogenic factors, offering a more realistic representation of ecological interactions. We established the model's mathematical well-posedness by proving the positivity and boundedness of solutions. Local and global stability conditions for the system's equilibria were derived, and the occurrence of Hopf bifurcation was analyzed to identify conditions under which periodic oscillations emerge. Furthermore, we explored the optimal harvesting strategy by deriving the Maximum Sustainable Yield under simplified assumptions. Numerical simulations confirmed the theoretical findings and demonstrated the significant influence of wind intensity, harvesting effort, and group defense on system stability. Notably, strong wind flow and moderate harvesting can stabilize the system, while excessive prey defense or harvesting may lead to predator extinction. These results highlight the delicate balance required to maintain biodiversity and ecosystem stability. The model has practical implications for ecological management and conservation, particularly in systems where environmental variability and human exploitation are prominent. Our model can be applied to study real-world predator-prey systems, such as bison and wolves or lions and wildebeest , etc [11-14]. In these relationships, bison serve as prey for wolves; wildebeest serve as prey for lions. Research indicates that bison utilize a group defense strategy to help mitigate wolf attacks. On the other hand, wolves, functioning as predators, face intraspecific competition, which can lead to behaviors like cannibalism within their species. Simultaneously, windy conditions can significantly impact predation success across various species [4,5]. Lion hunting is less successful in capturing wildebeest during windy conditions. Future research could extend this model by incorporating periodic environmental fluctuations, spatial heterogeneity, or alternative functional responses to further enhance its ecological relevance.

Conflicts of interest

The authors state that there are no conflicts of interest.

References

[1] McVicar, T. R., Roderick, M. L., Donohue, R. J., Li, L. T., Van Niel, T. G., Thomas, A., Grieser, J., Jhajharia, D., Himri, Y., Mahowald, N. M., Mescherskaya, A.V., Kruger, A. C., Rehman, S., and Dinpashoh, Y., Global review and synthesis of trends in observed terrestrial near-surface wind speeds: Implications for evaporation, Journal of Hydrology, vol. 416–417, pp. 182–205, Jan. 2012. https://doi.org/10.1016/j.jhydrol.2011.10.024

[2] Cherry, M. J. and Barton, B. T., Effects of wind on predator-prey interactions, Food Webs, vol. 13, pp. 92–97, Dec. 2017. https://doi.org/10.1016/j.fooweb.2017.02.005

[3] Liu, S., Zhao, and Q., Niu, X., Effect of water temperature on the dynamic behavior of phytoplankton - zooplankton model, Applied Mathematics and Computation, vol. 378, Aug. 2020, Art. no. 125211. https://doi.org/10.1016/j.amc.2020.125211

[4] Barman, D., Roy, J., and Alam, S., Impact of wind in the dynamics of prey–predator interactions, Mathematics and Computers in Simulation, vol. 191, pp. 49–81, Jan. 2022. https://doi.org/10.1016/j.matcom.2021.07.022

[5] Barman, D., Kumar, V., Roy, J., and Alam, S., Modeling wind effect and herd behavior in a predator–prey system with spatiotemporal dynamics, The European Physical Journal Plus, vol. 137, Aug. 2022, Art. no. 950. https://doi.org/10.1140/epjp/s13360-022-03133-4

[6] Takyi, E., Cooper, K., Dreher, A., and Mccrorey, C., Dynamics of a predator - prey system with wind effect

and prey refuge, Journal of Applied Nonlinear Dynamics, vol. 12, iss. 3, pp. 427–440, 2023. https://doi.org/10.5890/JAND.2023.09.001

[7] Chakraborty, S., Pal, S., and Bairagi, N., Predator–prey interaction with harvesting: mathematical study with biological ramifications, Applied Mathematical Modelling, vol. 36, iss. 9, pp. 4044–4059, Sep. 2012. https://doi.org/10.1016/j.apm.2011.11.029

[8] Pratama, R. A., Ruslau, M. F. V., Suryani, D. R., and Meirista, E., Optimal harvesting and stability of predator-prey model with Holling type ii predation respon function and stage-structure for predator, Journal of Physics: Conference Series, vol. 1569, iss. 4, 2020, Art. no. 042067. https://doi.org/10.1088/1742-6596/1569/4/042067

[9] Luo, J. and Zhao, Y., Stability and bifurcation analysis in a predator–prey system with constant harvesting and prey group defense, International Journal of Bifurcation and Chaos, vol. 27, 2017, Art. no. 1750179. https://doi.org/10.1142/S0218127417501796

[10] Hass, C. C. and Valenzuela, D., Anti-predator benefits of group living in white-nosed coatis (*Nasua narica*), Behavior Ecology and Sociobiology, vol. 51, pp. 570–578, Mar. 2002. https://doi.org/10.1007/s00265-002-0463-5

[11] Carbyn Ludwig N., Trottier T., Responses of bison on their calving grounds to predation by wolves in Wood Buffalo National Park, Canadian Journal of Zoology, vol. 65, iss. 8, pp. 2072–2078, 1987. https://doi.org/10.1139/z87-317

[12] MacNulty Daniel R, Mech LD, and Smith Douglas W., A proposed ethogram of large-carnivore predatory behavior, exemplified by the wolf, J. Mammal, vol. 88, iss. 3, pp. 595–605, 2007. https://doi.org/10.1644/06-MAMM-A-119R1.1

[13] Laundré John W, Hernández Lucina, and Altendorf Kelly B., Wolves, elk, and bison: reestablishing the "landscape of fear" in Yellowstone National Park, Canadian Journal of Zoology, vol. 79, no. 8, pp. 1401–1409, Aug. 2001. https://doi.org/10.1139/z01-094

[14] Hernández Lucina and Laundré John W., Foraging in the 'landscape of fear' and its implications for habitat use and diet quality of elk Cervus elaphus and bison Bison bison, Wildlife Biology, vol. 11, iss. 3, pp. 215 –220, Sep. 2005. https://doi.org/10.2981/0909-6396(2005)11[215:FITLOF]2.0.CO;2